Towards Standardizing Affine Frequency Division Multiplexing (AFDM) for Future Wireless Networks

Qu Luo, *Member, IEEE,* Lixia Xiao, *Member, IEEE,* Pei Xiao, *Senior Member, IEEE,* Zilong Liu, *Senior Member, IEEE,* Yin Xu, *Member, IEEE,* Qihao Peng, *Member, IEEE,* Zeping Sui, *Member, IEEE,* Hee Wook Kim, *Member, IEEE,* and Hüseyin Arslan, *Fellow, IEEE*.

***Abstract*—Affine frequency division multiplexing (AFDM) has emerged as a compelling waveform candidate for future wireless networks, owing to its strong resilience to doubly selective channels and its ability to enable the seamless integration of communication and sensing functionalities. Against this context, this article provides a systematic study of AFDM from a standardization perspective. We first introduce the principles of AFDM and discuss the major considerations involved in waveform standardization. We then examine the backwards compatibility of AFDM with 4G/5G multi-numerology frameworks and their anticipated evolution, frequency-modulated continuous-wave (FMCW) radar waveforms, and long-range (LoRa) modulation, demonstrating that AFDM can be incorporated into legacy processing chains with limited modification. Key standardization-critical capabilities are further discussed, including multiple-antenna and multi-user support, and peak-to-average power ratio (PAPR). Finally, we investigate the potential of AFDM in several emerging scenarios, including non-terrestrial networks (NTN), integrated sensing and communications (ISAC), vehicle-to-everything (V2X), and underwater acoustic (UWA) communications, whereby severe delay-Doppler dispersion places stringent demands on waveform robustness. Through these explorations, it is shown that that AFDM represents a timely and compelling technology for future wireless networks.**

***Index Terms*—Affine frequency division multiplexing (AFDM), standardization, NR multi-numerology, FMCW, NTN, ISAC, V2X and UWA.**

I. Introduction

FUTURE wireless networks are expected to support an intelligent, highly interconnected society with tightly integrated communication, sensing, and computing across terrestrial and non-terrestrial platforms [1], [2]. The IMT-2030 vision anticipates the sixth-generation (6G) system delivering peak data rates beyond 1 Tbps, sub-millisecond latency, connection densities up to 10^8 devices/km^2, and reliable operation at mobility speeds exceeding 1000 km/h [3]. A defining requirement is to achieve ubiquitous connectivity in challenging high-mobility scenarios, including high-speed railways, unmanned aerial vehicles (UAVs), vehicle-to-everything (V2X) communications , and integrated terrestrial and non-terrestrial networks (NTNs). Achieving these ambitious targets demands fundamental innovation at the physical layer (PHY), with multicarrier waveform design playing a central role [4]. Orthogonal frequency division multiplexing (OFDM) has long served as the dominant waveform in the fourth-generation long-term evolution (4G LTE) and the fifth-generation new radio (5G NR) systems, owing to its efficient multipath mitigation, flexible resource allocation, and low-complexity frequency-domain equalization. However, in doubly dispersive channels, Doppler shifts destroy subcarrier orthogonality and induce severe inter-carrier interference (ICI), significantly degrading transmission reliability [1]. Besides, in high frequency bands (e.g., millimeter-wave or even THz bands), OFDM generally suffers from significantly higher phase noise and carrier frequency offset, leading to further increase of ICI. These limitations have motivated an active search for alternative waveforms and waveform enhancements that are inherently more resilient high mobility, channel dynamics, and hardware impairments.

Among the emerging waveform candidates for highly dynamic wireless environments, affine frequency division multiplexing (AFDM) has recently attracted significant attention [1], [2], [5]. AFDM maps data symbols onto orthogonal chirp subcarriers through the inverse discrete affine Fourier transform (IDAFT), and introduces two tunable chirp parameters, c_1 and c_2, to provide additional flexibility in waveform design. With appropriate parameter configuration matched to the channel delay-Doppler spread, AFDM yields a quasi-static and separable effective channel representation in the DAFT domain, thus can achieve full diversity over doubly dispersive channels. Moreover, AFDM generalizes OFDM and orthogonal chirp division multiplexing (OCDM) as special cases, offering a unified waveform framework [1]. Its transceiver can be implemented by augmenting a conventional FFT-based architecture with low-complexity pre- and post-chirp operations. Owing to these advantages, organizations such as the University of Surrey, ETRI, and Shanghai Jiao Tong University have proposed AFDM as a complementary waveform to OFDM in 3GPP TSG-RAN meetings (e.g. R1-

Qu Luo, Pei Xiao and Qihao Peng are with 5G & 6G Innovation Centre, University of Surrey, Guildford, GU2 7XH, UK. (e-mail: q.u.luo, p.xiao, q.peng @surrey.ac.uk).

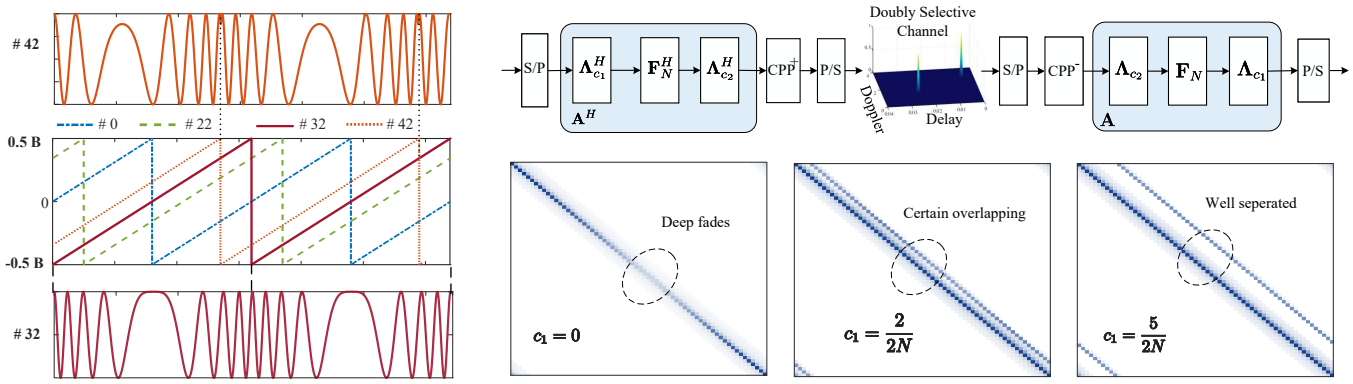
Lixia Xiao is with Research Center of 6G Mobile Communications, School of Cyber Science and Engineering, Huazhong University of Science and Technology, Wuhan 430074, China (e-mail:lixiaxiao@hust.edu.cn.)

Zilong Liu and Zeping Sui are with the School of Computer Science and Electronics Engineering, University of Essex, Colchester CO4 3SQ, U.K. (e-mail: zilong.liu@essex.ac.uk,zepingsui@outlook.com).

Yin Xu is with the School of Information Science and Electronic Engineering, Shanghai Jiao Tong University, Shanghai 200240, China, (e-mail: xuyin@sjtu.edu.cn).

Hee Wook Kim is with the Satellite Communication Research Division, Electronics and Telecommunications Research Institute (ETRI), Daejeon 34164, South Korea (email: prince304@etri.re.kr).

H. Arslan is with the Department of Electrical and Electronics Engineering, Istanbul Medipol University, Istanbul, 34810, Turkey, (e-mail: huseyinarslan@medipol.edu.tr).



(a) AFDM wrapped subcarriers

(b) AFDM modulation block diagram and its effective channel representation

Fig. 1: Illustration of AFDM Principles: (The AFDM subcarriers with $N = 64$ and $c_1 = \frac{1}{N}$); (b) AFDM modulation and its effective channel representation fore $N = 64$, assuming a two-path channel with normalized delay-Doppler pairs $(0, 0.5)$, $(2, 0.1)$, respectively. S/P and P/S denote serial-to-parallel and parallel-to-serial conversion, respectively.

2604486, R1-2602803 and R1-2602781) [6].

Despite the extensive research attention devoted to AFDM, it has not yet been systematically studied from a standardization perspective. This article addresses this gap by examining AFDM as a practical waveform candidate for future wireless networks. To become a viable candidate for future wireless standards, a waveform must be assessed from a broader system and ecosystem perspective, including backwards compatibility with legacy systems, support for multiple antennas and multi-user transmission, energy and spectral efficiency, implementation complexity, and emerging applications such as NTN, integrated sensing and communications (ISAC), vehicle-to-everything (V2X), and underwater acoustic (UWA) communications. *In a nutshell, we investigate how AFDM can be seamlessly integrated into existing frameworks, what critical capabilities it offers, and where its most promising application opportunities lie.*

II. AFDM for Future Wireless Networks

A. Preliminaries of AFDM

Unlike conventional OFDM, which relies on sinusoidal subcarriers, AFDM is built upon chirp subcarriers whose instantaneous frequency varies linearly with time. For an AFDM symbol of N subcarriers, the nth discrete-time chirp subcarrier is expressed as $\psi_n[m] = \frac{1}{\sqrt{N}} e^{j2\pi\left(c_1 n^2 + c_2 m^2 + \frac{nm}{N}\right)}, \quad m, n = 0, \ldots, N-1$. Here, c_1 imposes a uniform chirp rate across N subcarriers and c_2 introduces subcarrier-dependent initial phases. Notably, OFDM and OCDM are both special cases of AFDM, corresponding to $c_1 = c_2 = 0$ and $c_1 = c_2 = -1/(2N)$, respectively. Therefore, as a natural generalization of OFDM, AFDM preserves strong backwards compatibility with legacy infrastructures. An important feature of the AFDM chirp subcarrier structure is spectral wrapping upon digital sampling, as shown in Fig. 1(a). Denoting the system bandwidth by B and the symbol duration by $T = N/B$, each AFDM subcarrier is obtained by sampling the continuous-time chirp signal $K_n(t) = \frac{1}{\sqrt{N}} \mathrm{e}^{j2\pi(\frac{c_1 N^2}{T^2} t^2 + \frac{nt}{T} + c_2 n^2)}$ at the sampling rate of B. When $c_1 > 1/(2N)$, the instantaneous bandwidth of $K_n(t)$ exceeds the Nyquist rate B, and digital sampling therefore folds the spectrum periodically into the interval $[-0.5B, 0.5B]$, leading to the wrapped subcarriers. A particularly structured case arises when $c_1 = Q/(2N)$ for some integer Q. Under this condition, the $\frac{N}{2}$th subcarrier undergoes exactly Q spectral sweeps within one symbol duration, whereas the remaining subcarriers complete exactly $Q + 1$ sweeps [1], [5].

A key advantage of AFDM is its ability to exploit channel diversity over doubly dispersive channels. By properly selecting c_1, different delay-Doppler paths may occupy non-overlapping diagonals in the effective channel matrix, each path contributes a unique band-diagonal component in the DAFT domain. The resulting sparse, structured representation enables efficient suppression of both inter-symbol interference (ISI) and ICI even under severe delay and Doppler spreads, as shown in Fig. 1(b).

B. Standardization Considerations

The aforementioned advantages make AFDM a highly promising waveform candidate for future wireless networks. Standardizing AFDM, however, requires a systematic evaluation that extends well beyond error-rate performance. In general, waveform standardization involves a broad set of considerations, including backwards and forwards compatibility, multi-antenna and multi-user support, spectral efficiency, coverage, peak-to-average power ratio (PAPR), and scheduling flexibility. Among these, backwards compatibility is a major consideration, since a practical waveform should integrate smoothly into the existing 5G framework, including downlink cyclic-prefix OFDM (CP-OFDM) and uplink discrete Fourier transform-spread OFDM (DFT-s-OFDM), without radical changes to the numerology, resource grid, or transceiver architecture. Meanwhile, future networks are expected to support emerging applications such as NTN, ISAC, V2X communications, and UWA communications, many of which generally operate under severe delay and Doppler dispersion.

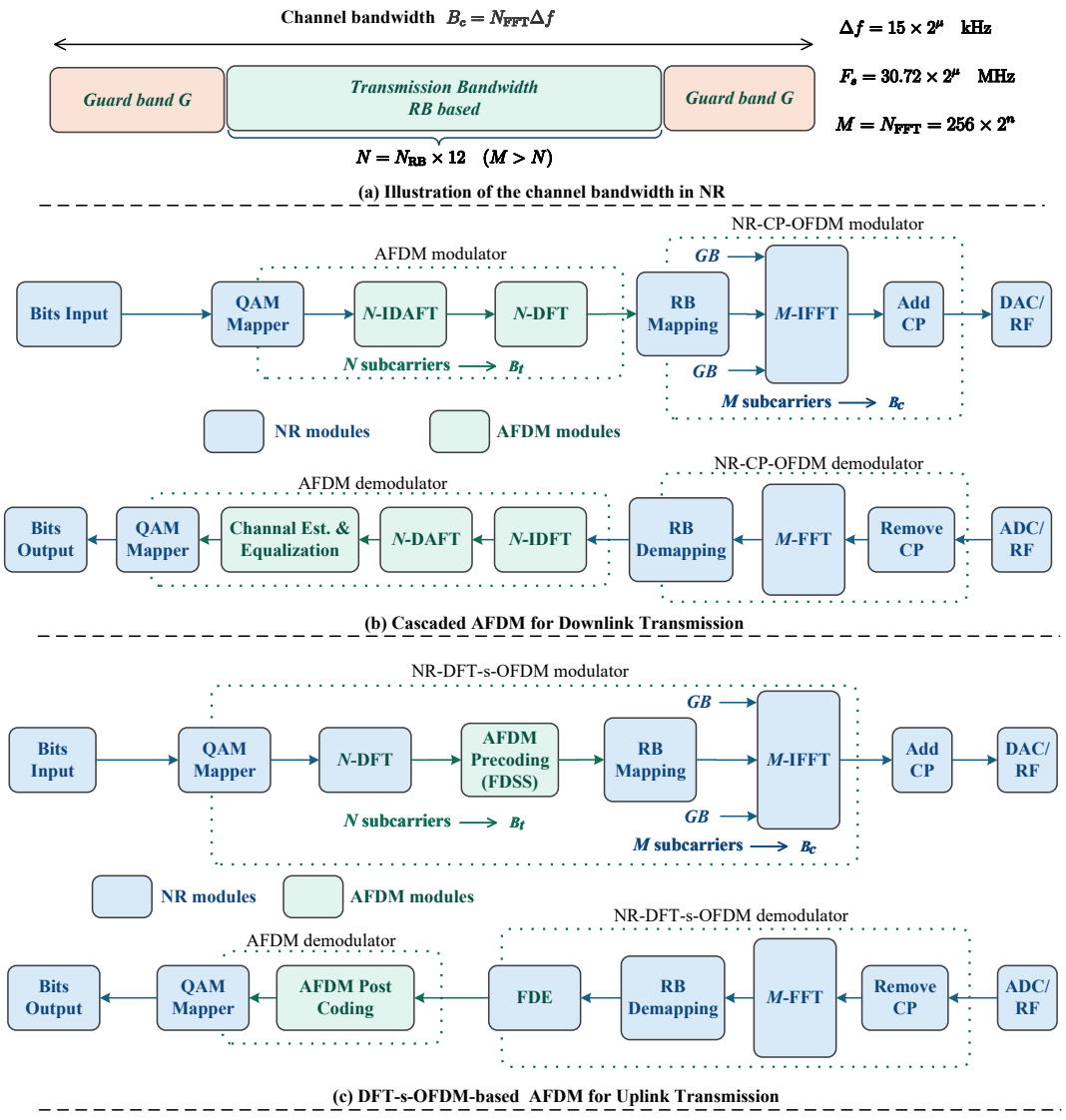


Fig. 2: Downlink and Uplink backwards Compatibility with 5G NR Numerology, where $c_1 = \frac{Q}{2N}, Q \in \mathbb{Z}$ (DAC: digital-to-analog converter; CP: cyclic prefix; RF: radio frequency; QAM: quadrature amplitude modulation; GB: Guard band.).

In this regard, AFDM represents a timely and compelling opportunity.

III. Backwards Compatibility of AFDM

A. Downlink Backwards Compatibility with 5G NR Numerology

One of the defining features of NR is its flexible numerology, which enables scalable waveform parameterization for diverse deployment scenarios. Specifically, NR adopts subcarrier spacings of $\Delta f = 15 \times 2^{\mu}$ kHz, where $\mu \in \{0, 1, 2, 3, 4\}$ denotes the numerology index, as specified in TS 38.101 and TS 38.104 [7], supporting subcarrier spacings up to 240 kHz. To accommodate these numerologies within a unified framework, NR retains the legacy reference sampling rate of 30.72 Msps, corresponding to a 2048-point OFDM system with 15 kHz subcarrier spacing. The basic sampling rate scales with numerology as $F_s = 30.72 \times 2^{\mu}$ Msps.

Although the N-point IDAFT can be decomposed into an N-point IFFT kernel followed by low-complexity pre-chirp and post-chirp operations in the digital baseband, as shown in Fig. 1(b), enabling backwards-compatible integration of AFDM into NR systems with multi-numerology operation requires addressing several practical issues. First, in 4G/NR downlink transmission, the channel bandwidth is given by $B_c = B_t + G = N_{\text{FFT}}\Delta f$, which consists of both guard band and effective transmission bandwidth, as shown in Fig. 2(a). Second, practical transmitters employ digital interpolation and filtering before the DAC to satisfy spectral emission requirements. This generally requires the sampling bandwidth to be larger than the occupied signal bandwidth, thereby providing sufficient transition bands for suppressing interpolation-induced spectral aliasing. In OFDM, these transition and guard bands are realized by nulling edge subcarriers before the N_{FFT}-point IFFT. In AFDM, however, each DAFT-domain symbol

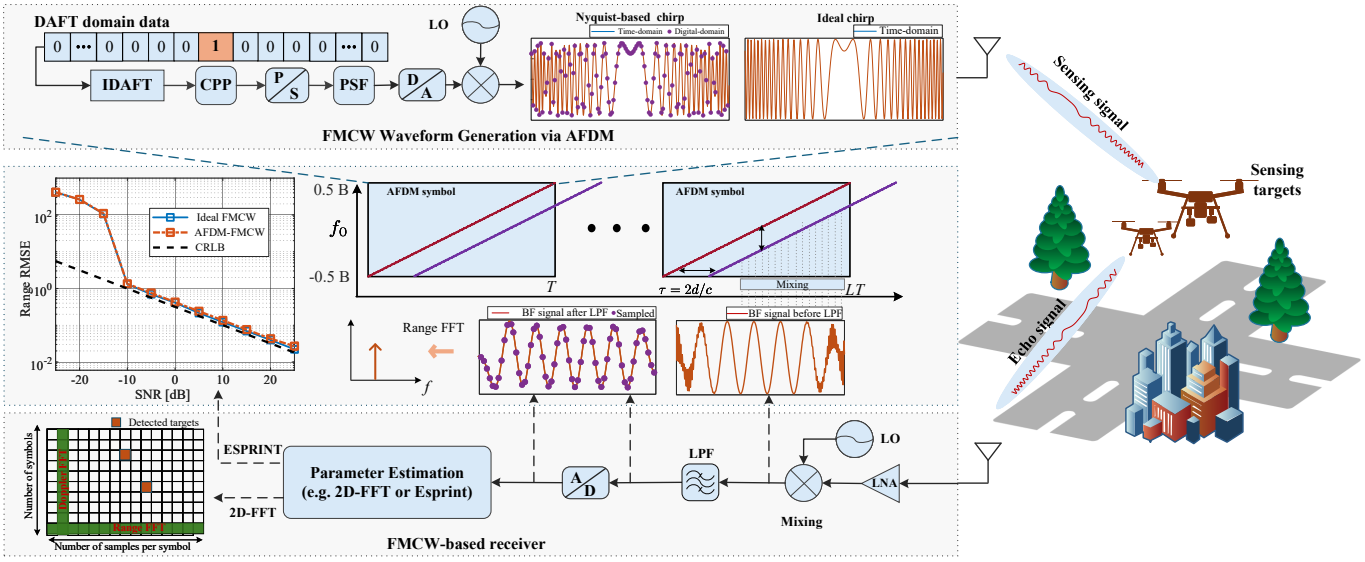


Fig. 3: Illustration of the backwards compatibility of AFDM with FMCW radar. The simulation parameters are $N = 512$, subcarrier spacing $= 15$ kHz, number of chirps $= 64$, $c_1 = c_2 = 1/(2N)$, and carrier frequency $f_c = 6$ GHz.

spans the entire bandwidth, so nulling DAFT-domain symbols does not create guard bands in the same manner.

Fig. 2(b) illustrates the cascaded AFDM-NR waveform architecture for downlink transmissions. AFDM modulation is first applied over the transmission bandwidth B_t via the IDAFT, followed by an additional FFT module and the conventional NR CP-OFDM processing chain. Compared with conventional CP-OFDM, this implementation therefore introduces two additional FFT/IFFT operations. The resulting FFT-domain AFDM signal is mapped onto the active NR resource blocks (RBs)[1], while edge subcarriers are nulled to form the guard band. In this way, AFDM occupies a transmission bandwidth of B_t, while the subsequent CP-OFDM modulator determines the overall channel bandwidth. For example, for a 15-MHz NR channel bandwidth with $\Delta f = 30$ kHz, TS 38.104 specifies 38 resource blocks and a minimum guard band of 645 kHz on each side, yielding $N_{\text{IDAFT}} = 38 \times 12$. To align with NR sampling-rate scaling, $N_{\text{FFT}} = 512$ can be adopted, corresponding to $f_s = 15.36$ Msps. This design enables flexible implementation of AFDM within the NR downlink framework.

B. Uplink backwards Compatibility with 5G NR Numerology

In the uplink, AFDM can be integrated in a backwards-compatible manner within the legacy DFT-s-OFDM architecture adopted by both 4G LTE and 5G NR. In particular, the chirp operation in the time domain can be equivalently realized as multiplicative spectral shaping in the frequency domain [8]. AFDM can thus be embedded into DFT-s-OFDM by inserting a properly designed DFT-domain precoding matrix [9]. This approach is highly compatible with existing 4G/5G uplink transmission, since a similar frequency-domain precoding operation has already been standardized in 5G NR for PAPR reduction in DFT-s-OFDM systems, termed frequency-domain spectral shaping (FDSS). By configuring the FDSS coefficients according to the AFDM precoding coefficients, AFDM can therefore be implemented within the existing NR DFT-s-OFDM framework, as illustrated in Fig. 2(c). AFDM-oriented FDSS can thus be viewed as a structured extension of existing shaping methods, where the coefficients are designed not only for spectrum containment but also for realizing the target chirp-domain waveform. Since AFDM is incorporated as an FDSS-based processing block rather than a new modulation chain, the legacy uplink architecture, including DFT spreading, resource mapping, OFDM modulation, and CP insertion, can be retained with minor modification. In addition, the AFDM-oriented FDSS coefficients can be deterministically generated from the configured chirp parameter c_1, thereby avoiding the need to signal the individual FDSS coefficients and resulting in only limited additional signaling overhead. Moreover, AFDM naturally operates under the NR multi-numerology framework, reusing the same scalable FFT sizes, symbol durations, CP lengths, and sampling rates, enabling coexistence with legacy DFT-s-OFDM across different bandwidth parts and deployment scenarios.

In a nutshell, AFDM can be interpreted not as a replacement for the existing NR framework, but as an enhanced signal-shaping mode embedded into existing transmitters. More importantly, multi-RAT spectrum sharing (MRSS) is being actively considered in 3GPP as an important mechanism for enabling spectrum coexistence and a smooth migration from 5G to 6G. MRSS, together with the proposed NR-compatible downlink and DFT-s-OFDM/FDSS-based uplink implementations, provides a promising pathway for AFDM to coexist with legacy NR waveforms within a common numerology and resource-grid framework.

[1] An RB is the minimum scheduling unit in NR, consisting of 12 subcarriers.

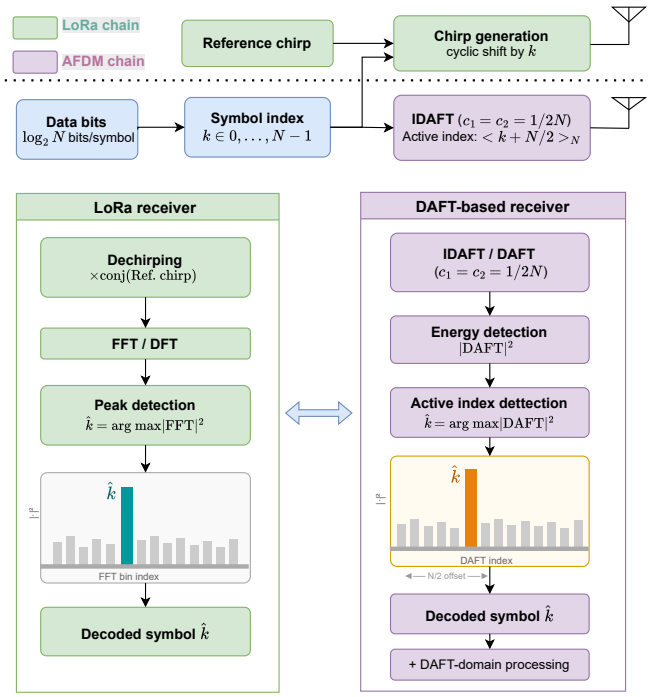


Fig. 4: Illustration of the conventional LoRa modulation and the proposed AFDM-based LoRa transceiver.

C. Backwards Compatibility with Radar-centric Waveform

Chirp signals are well known for their *pulse compression* capability and are therefore widely used in conventional radar systems, particularly frequency-modulated continuous-wave (FMCW) radar [10]. AFDM can generate an FMCW-compatible chirp waveform under a specific parameter configuration, allowing the conventional dechirping-based FMCW receiver architecture to be reused. Specifically, when the $N/2$-th subcarrier is activated and $c_1 = \frac{1}{2N}$, the generated discrete chirp spans from $-0.5B$ to $0.5B$ over a chirp duration T with chirp rate $\alpha = B/T$, which is compatible with the discrete FMCW waveform, as illustrated in Fig. 3. At the receiver, the echo is mixed with a reference chirp to produce the beat-frequency (BF) signal at $f_{\mathrm{BF}} = \alpha\tau$, where τ is the propagation delay.

Traditional FMCW radars operate in the analog domain via voltage-controlled oscillators, whereas AFDM generates chirps digitally through DAFT-domain modulation—a Nyquist-sampled discrete-time realization of FMCW [11]. Although slight distortion may appear near band edges compared with ideal analog FMCW, these distortion components are shifted to high frequencies after dechirping (well above the desired BF term $\alpha\tau$) and are effectively removed by subsequent low-pass filtering (LPF), as shown in Fig. 3. Consequently, AFDM-FMCW achieves sensing performance close to conventional FMCW and near the Cramér–Rao lower bound (CRLB). This compatibility provides useful insights for future 6G ISAC standardization, particularly for V2X scenarios where FMCW radar is widely adopted.

D. Backwards Compatibility with LoRa Waveform

LoRa is a chirp spread spectrum (CSS) waveform widely used in low-power wide-area networks (LPWANs) for Internet-of-Things (IoT) applications. CSS encodes information through cyclic shifts of a reference linear chirp with each symbol corresponds to one of N possible chirp states, carrying $\log_2 N$ bits. When AFDM parameters are set to $c_1 = c_2 = \frac{1}{2N}$, the active DAFT-domain index becomes exactly the data-carrying symbol position in conventional LoRa. As conventional LoRa does not employ a prefix, the AFDM CPP length should be configured to zero to maintain strict waveform compatibility. Hence, LoRa signaling can be interpreted as a single-active-index chirp mode within AFDM, as shown in Fig. 4.

This equivalence naturally enables practical backward compatibility with conventional LoRa transceivers, as shown in Fig. 4. The receiver can either reuse the conventional LoRa demodulation chain (dechirping followed by FFT-domain peak detection) or perform detection directly in the AFDM DAFT domain by identifying the active index position. The former preserves the existing LoRa receiver architecture, whereas the latter enables native AFDM-domain processing. This dual interpretation supports cross-domain processing between time and DAFT domains, offering enhanced robustness in high-mobility scenarios such as NTN LPWANs applications. From a standardization perspective, this connects AFDM to the existing LPWAN and narrowband IoT ecosystem.

E. Other Important Considerations for Standardization

Beyond the compatibility aspects discussed above, waveform standardization also requires evaluation across multiple performance dimensions, including support to multiple-input and multiple output (MIMO) and multiple access (MA), and energy efficiency. Therefore, this subsection focuses on these three key capabilities of AFDM.

1) Multiple access

MA capability is an important consideration in waveform standardization. Unlike the downlink where transmission is centrally coordinated at the base station, uplink access needs to accommodate independently transmitted user signals under heterogeneous channel conditions and asynchronous transmissions. AFDM can support uplink MA along the following two complementary directions.

Native AFDM-oriented MA: Similar to DFT-s-OFDM, a native DAFT-spread affine frequency division multiple access (DAFT-s-AFDMA) scheme was proposed in [12], where multiple users share the available chirp subcarriers and each user performs DAFT-domain spreading before resource mapping and AFDM modulation. By spreading each user's symbols over the allocated DAFT-domain resources, this structure is more robust to localized multi-user interference caused by heterogeneous delay-Doppler effects. Additionally, the DAFT spreading introduces a configurable pre-chirp parameter (c_2), providing an extra degree of freedom for PAPR reduction.

MA build upon DFT-s-OFDM: Another attractive approach is to support AFDM-based uplink access through backwards-compatible integration into the existing 5G NR uplink frame-

TABLE I: Achieved Net Gain of AFDM.

UE Speed	Benchmark Waveform	Net Gain @10% BLER
3 km/h	CP-OFDM	0.8 dB
	DFT-s-OFDM	0.6 dB
500 km/h	CP-OFDM	3.0 dB
	DFT-s-OFDM	2.5 dB
1500 km/h	CP-OFDM	5.2 dB
	DFT-s-OFDM	4.5 dB

Carrier frequency: 4 GHz, $N = 512$, $c_1 = c_2 = 2/N$, subcarrier spacing: 30 kHz, channel model: TDL-A, modulation: QPSK, PA model: Rapp model, channel code: 5G NR LDPC with code length and rate of 512 and $4/5$, respectively.

work. As NR already adopts DFT-s-OFDM for uplink transmission, and AFDM can be naturally realized through FDSS-based DFT-s-OFDM processing, as shown in Fig. 2, different users may employ user-specific FDSS coefficients to induce the desired chirp-domain structure, followed by DFT spreading and subcarrier mapping prior to OFDM modulation. This allows the existing scheduling and resource allocation mechanisms to remain largely unchanged, while naturally supporting coexistence of legacy DFT-s-OFDM users (e.g., low-mobility) and AFDM-enabled users (e.g., high-mobility) within a common uplink framework.

Overall, the native AFDM-oriented MA scheme proposed in [12] relies on the conventional DAFT/IDAFT-based AFDM transceiver, whereas the proposed DFT-s-OFDM-based MA scheme is intended to provide better compatibility with the existing NR uplink structure.

2) PAPR

PAPR is a key concern in waveform standardization, particularly for uplink transmission due to UE power amplifier constraints. In recent 3GPP discussions on low-PAPR uplink waveforms, the evaluation focuses on the *Net Gain* criterion under the same spectral efficiency as the reference waveform:

$$G_{\text{net}} = G_{\text{tx}} - \Delta\gamma_{10\%\text{BLER}}, \tag{1}$$

where G_{tx} denotes the transmit-power gain relative to the reference waveform, and $\Delta\gamma_{10\%\text{BLER}}$ denotes the SNR degradation at 10% block error rate (BLER). Under this model, Net Gain thus reflects the transmit-power gain jointly with the BLER-related SNR loss, rather than a standalone PAPR reduction. A realistic PA model and PA back-off should also be incorporated when evaluating such gains.

AFDM is attractive in that its PAPR reduction can be achieved along the following two directions. First, both native AFDM and its DFT-s-OFDM-based realization remain compatible with existing low-PAPR techniques (PTS, tone reservation, etc.). Second, the chirp parameter c_2 can generate different DAFT-domain phase rotations, leading to signals with different peak characteristics—analogous to selected mapping (SLM) in OFDM but induced by intrinsic chirp parameterization [12], [13]. Table I compares the Net Gain of AFDM over CP-OFDM and of DAFT-s-AFDM over DFT-s-OFDM, respectively, using a memory-based polynomial PA model. As observed, the Net Gain of AFDM over OFDM becomes more prominent as mobility increases.

3) MIMO

MIMO-AFDM systems process signals in a joint spatial-Affine (SAF) domain, combining AFDM's delay-Doppler resilience with MIMO spatial gains. The end-to-end relation in the SAF domain is $\mathbf{y} = \sum_{i=1}^{P}(\mathbf{H}_{\text{S},i} \otimes \mathbf{H}_{\text{AF},i})\mathbf{Q}\mathbf{x} + \mathbf{w}$, where the per-path SAF channel is the Kronecker product of spatial ($\mathbf{H}_{\text{S},i}$) and affine-domain ($\mathbf{H}_{\text{AF},i}$) channel matrices [14]. Since spatial and affine domains capture inherently different physical characteristics, precoding must be designed jointly across both. In single-user scenarios, the Kronecker structure enables a low-complexity LOS-based approximation requiring only LOS-path CSI at the transmitter [14]. In multi-user settings, weighted MMSE extends naturally to the SAF domain to suppress inter-user interference across spatial, delay, and Doppler dimensions jointly.

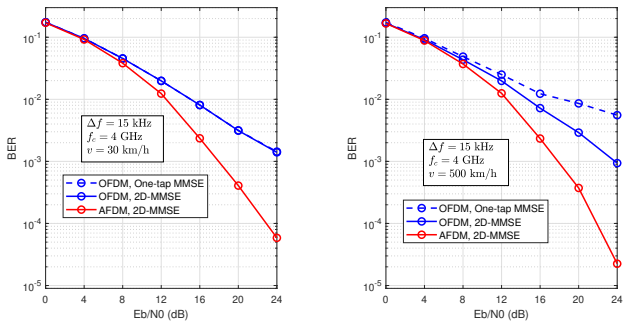
IV. Standardizing AFDM Towards Emerging Applications

AFDM is particularly attractive in scenarios where robustness to delay–Doppler dispersion is of central importance. In this regard, AFDM exhibits strong potential in several emerging applications, including NTN, ISAC, V2X, and UWA communications. This sections discuss how the intrinsic properties of AFDM can be exploited to meet/support these requirements and evolution trends of these emerging application domains.

A. NTN

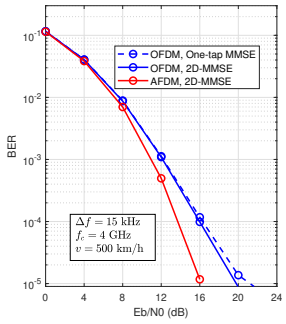
NTN are a key enabler for ubiquitous connectivity in next-generation wireless networks. Typical NTN platforms include UAVs, high-altitude platforms, aircraft, and satellites, all inherently associated with high-mobility environments. In satellite communications, NTN links are further characterized by large propagation delays and delay variations. To cope with Doppler effects, legacy OFDM-based solutions mainly rely on two mechanisms: 1) increasing the subcarrier spacing at the cost of shorter symbol duration and reduced robustness to long delay spread; and 2) estimating and compensating the dominant Doppler component while treating residual Doppler as interference. However, this strategy becomes increasingly ineffective in downlink NTN scenarios where multipath propagation is prevalent and different paths may experience distinct delay-Doppler shifts, leading to non-negligible residual interference. Fig. 5 compares the BER of AFDM and OFDM over the 3GPP NTN-TDL channel models specified in TR 38.901 and TR 38.821 [7], where NTN-TDL-A/B corresponds to non-LOS scenarios and NTN-TDL-C/D to LOS-dominant conditions. The "OFDM, One-tap" curves employ conventional one-tap linear MMSE equalization with dominant-path Doppler compensation, whereas the "2D-MMSE" curves employ block linear-MMSE equalization, as in [5]. In LOS-dominant scenarios, OFDM remains applicable when the dominant Doppler is accurately compensated. However, in richly scattered channels where different paths experience non-negligible delay-Doppler coupling, conventional Doppler compensation in OFDM may be ineffective.

Additionally, the initial access procedure in high-mobility satellite networks itself is a major challenge for OFDM-based systems. Random-access preambles must be detected under large delay uncertainty, strong Doppler shift, and Doppler

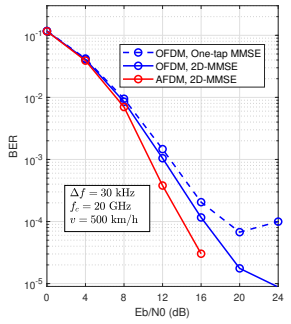


(a) 30 km/h, TDL-A

(b) 500 km/h, TDL-A



(c) 500 km/h, TDL-D



(d) 500 km/h, TDL-D

Fig. 5: BER comparisons of OFDM and AFDM over NTN-TDL channels, where $c_1 = c_2 = 2/N$. (The delay and power profiles of the first three taps for NTN-TDL-A are $\boldsymbol{\tau}_{\mathrm{A}} = [0,\ 38.2,\ 40.3]$ ns and $\mathbf{p}_{\mathrm{A}} = [-13.4,\ 0,\ -2.2]$ dB, and those for NTN-TDL-D are $\boldsymbol{\tau}_{\mathrm{D}} = [0,\ 3.5,\ 61.2]$ ns and $\mathbf{p}_{\mathrm{D}} = [-0.2,\ -18.8,\ -21.0]$ dB, respectively. The actual tap delays are obtained as $\tau_l = \tau_{l,\mathrm{norm}} \times \mathrm{DS}$, where DS denotes the root-mean-square delay spread, which is set to 100 ns. The complete model parameters can be found in [7]).

drift. Current NR NTN applies GNSS-based Doppler pre-compensation and Zadoff-Chu preamble sequences up to length 839 for roubust initial access. Nevertheless, reliable preamble detection remains challenging under large delay uncertainty, severe Doppler shift, and Doppler drift. By contrast, AFDM provides additional flexibility: its chirp waveform preserves favorable correlation characteristics, and the DAFT-domain representation facilitates separation of Doppler shifts, multipath delays, and their coupled dispersion, making it attractive for robust preamble detection in satellite scenarios.

B. ISAC

ISAC is widely recognized as an important capability for future wireless standards. Owing to its time-domain chirp pulse compression and DAFT-domain representation, AFDM provides several attractive advantages for ISAC applications [4]. In particular, AFDM supports both communication-centric ISAC, where communication signals are directly reused for sensing with maximum reuse of existing hardware, and sensing-centric ISAC, where deterministic chirp signaling is employed for radar sensing with compatibility to existing FMCW radar architectures. Fig. 6 summarizes the distinct features of these two schemes and provides a comprehensive comparison.

Communication-centric ISAC:

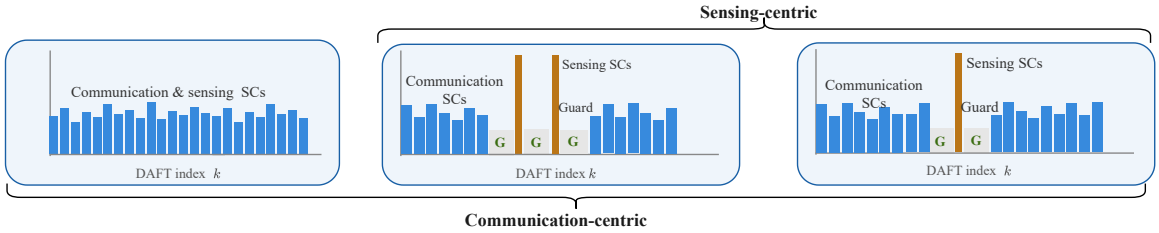
AFDM aided communication-centric sensing can be realized in the following two modes.

Full-subcarrier sensing: All AFDM chirp subcarriers simultaneously carry communication data and contribute to sensing. Target delay and Doppler are estimated via time-domain or DAFT-domain matched filtering after transmitted-data cancellation. This mode fully exploits the transmitted signal energy, thereby maximizing sensing SNR, and the DAFT-domain processing integrates naturally into the communication receiver chain. However, since sensing relies on knowledge of the transmitted data, this mode is mainly suitable for monostatic sensing with co-located transmitter and receiver, and requires effective full-duplex operation with sufficient antenna isolation to prevent ADC saturation caused by RF transmit-signal leakage.

Partial-subcarrier sensing: Since each AFDM chirp subcarrier occupies the entire bandwidth in time, sensing can be realized using only one or a few deterministic subcarriers while the remainder serve guard and communication purposes. This mode offers much greater flexibility in communication-sensing resource allocation, e.g., the sensing power can be adjusted according to requirements. It also alleviates the strict full-duplex requirement, as digital self-interference cancellation (SIC) can be implemented directly in the DAFT domain. Moreover, deterministic sensing subcarriers are promising for bistatic and multistatic scenarios, where they simplify waveform coordination and improve the scalability of distributed sensing.

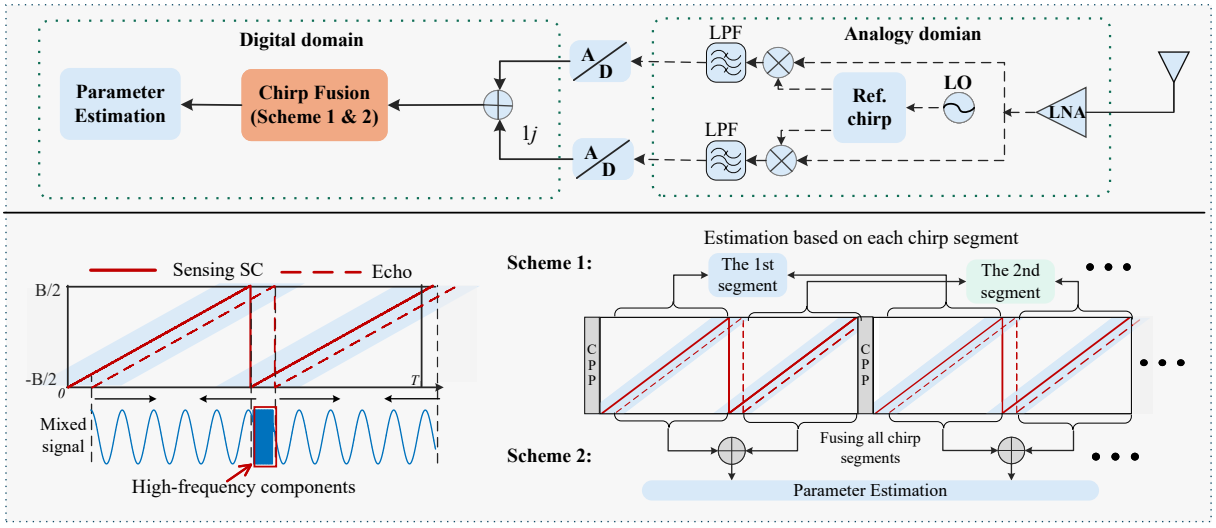
Sensing-centric ISAC:

In sensing-centric ISAC, dedicated chirp subcarriers (i.e., partial subcarriers) are designed primarily for sensing, while existing radar signal processing techniques and hardware architectures can be largely reused. As discussed in Subsection III-C, when AFDM is properly configured, the receiver can directly reuse the existing FMCW radar processing architecture. Fig. 6(b) shows the proposed AFDM-ISAC by using the $N/2$th subcarrier for sensing with $c_1 = 1/N$. Dechirping between communication subcarrier echoes and the reference signal also generates BF components. However, by introducing a proper guard band, the BF components from communication subcarriers can be effectively suppressed through LPF design. For larger chirp rates, i.e., $c_1 = Q/(2N), Q > 1$, , spectral wrapping occurs for AFDM chirp subcarriers in the frequency domain. This spectral wrapping, together with CPP insertion, introduces high-frequency components and phase discontinuities in the dechirped BF signal across the delay and Doppler dimensions. To address this issue while preserving compatibility with existing FMCW radar receivers, we propose two AFDM-oriented chirp-fusion schemes, as shown in Fig. 6(b). Fig. 6(c) further compares the root mean square error (RMSE) performance of the dechirp-based and communication-centric AFDM-ISAC schemes with that of OFDM-based schemes. Interested readers are referred to [15] for further details. The dechirping-based architecture is particularly attractive as it avoids full-duplex operation, suppresses local leakage

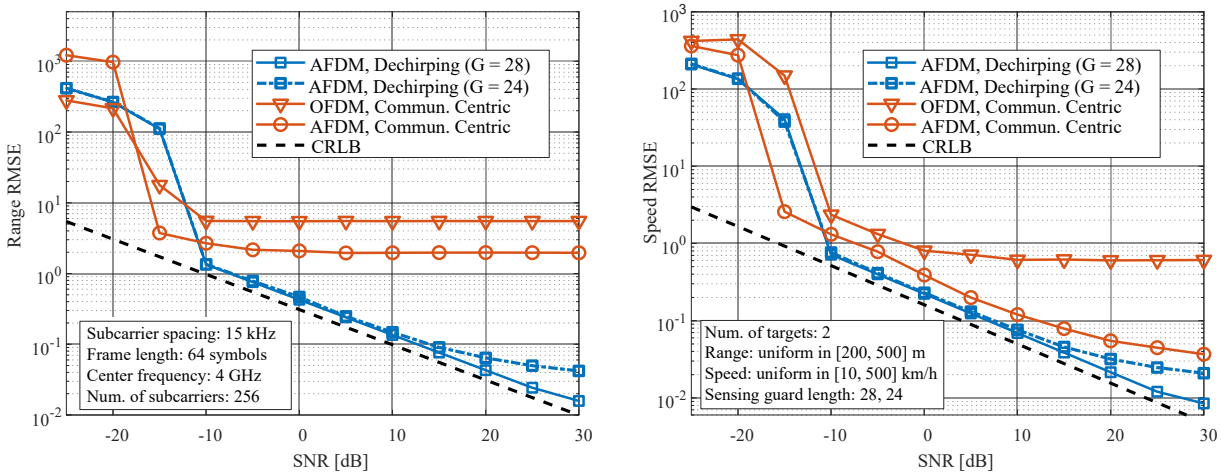


Property	Communication centric		Sensing-centric
Sensing subcarrier	All Communication SCs	Dedicated Sensing SCs+Guard SCs	Dedicated sensing SC+Guard SCs
Hardware reuse	Communication hardware	Communication hardware	FMCW radar hardware
Full-duplex burden	High	Moderate	No
Deployment	Monostatic	Monostatic & bistatic & multistatic	Monostatic & bistatic & multistatic
Sensing power	Full utilization	Partial (flexible)	Partial (flexible)
Sensing method	Time- or DAFT-domain MF	Time- or DAFT-domain MF	Time-domain dechirping
Suitable platform	BS	BS, UAV, Vehicle	BS, Vehicle, UAV, IoT

(a) A comparison of communication- and sensing-centric AFDM-ISAC systems.



(b) Illustration of sensing-centric AFDM-ISAC design.



(c) Range- and speed-RMSE comparisons of AFDM- and OFDM-ISAC, where $c_1 = c_2 = 1/N$ is considered.

Fig. 6: Illustration of communication- and sensing-centric AFDM-ISAC systems.

and communication-induced interference, and enables low-complexity implementation based on existing FMCW hardware. Hence, it is also well suited for resource-constrained sensing platforms with limited computational and hardware capabilities, such as sensing-enabled IoT devices and UAVs.

Overall, AFDM provides a distinctive ISAC standardization opportunity by supporting both communication-centric and sensing-centric modes within a unified chirp-based framework. For communication-centric ISAC, AFDM enables either full-band sensing to maximize sensing SNR or sparse sensing-subcarrier operation for improved flexibility and reduced full-duplex burden. For sensing-centric ISAC, AFDM offers strong compatibility with FMCW-based dechirping receivers, leading to hardware-efficient radar-oriented designs.

C. V2X

V2X systems demand low-latency, high-reliability information exchange among vehicles, infrastructure, pedestrians, and networks. AFDM's chirp-based structure and robustness in doubly dispersive channels make it well suited for synchronization signaling, random-access preamble design, and broadcast safety-message transmission under high-mobility V2X systems, aligning with the evolution of future vehicular PHYs. Additionally, AFDM's ISAC capability supports the growing need for environment sensing and positioning in vehicular networks. From a standardization perspective, AFDM offers a promising enhancement for extreme-mobility NR V2X sidelink, robust broadcast/control signaling, and future ISAC-enabled vehicular transmission.

D. UWA

UWA is another representative scenario in which AFDM may offer distinct advantages. UWA channels exhibit limited bandwidth, long propagation delay, large delay spread, severe Doppler distortion, and difficult synchronization, making reliable waveform design far more challenging than in terrestrial systems. AFDM is particularly suitable as a robust waveform for UWA control, discovery, and synchronization signaling. Its DAFT-domain structure is well matched to channels with strong multipath and non-negligible Doppler effects, improving waveform resilience in underwater links. In this context, AFDM is positioned not as a throughput-maximizing waveform, but as a robust PHY framework for foundational signaling and dependable low-rate communication under harsh underwater conditions.

V. Conclusion &Future Directions

This article has presented a systematic study of AFDM from a standardization perspective for future wireless networks. We demonstrated that AFDM exhibits strong backwards compatibility with the existing 5G NR downlink and uplink frameworks, as well as with FMCW radar waveforms, LoRa modulations, enabling its integration with minimal modifications to legacy processing chains. Key standardization-critical capabilities, including multiple access, PAPR reduction, and MIMO support, were evaluated, showing that AFDM provides both waveform-native design flexibility and compatibility with existing NR mechanisms. Furthermore, AFDM demonstrates strong potential in emerging scenarios, including NTN, ISAC, V2X, and UWA communications, where severe delay-Doppler dispersion places stringent demands on waveform robustness. These features position AFDM as a timely and compelling waveform candidate for future wireless standards.

Several open challenges remain for AFDM standardization. These including chirp-parameter configuration and reference-signal design compatible with existing NR mechanisms, initial access and ISAC waveform design for high-mobility scenarios (e.g., V2X, NTN, UWA), waveform coexistence with legacy systems, scalable MIMO and multi-user support, and hardware-oriented validation for practical deployment [1], [2].

References

[1] Q. Luo *et al.*, "Chirp-based OCDM and AFDM waveforms for 6G and beyond: Principles, recent advances, and future opportunities," Feb. 2026, authorea preprint, DOI: 10.22541/au.177145233.37871971/v1. [Online]. Available: https://www.authorea.com/doi/full/10.22541/au.177145233.37871971

[2] H. S. Rou, K. Roche Rayan Ranasinghe, V. Savaux, G. Thadeu Freitas de Abreu, D. González G., and C. Masouros, "Affine frequency division multiplexing (afdm) for 6g: Properties, features, and challenges," *IEEE Commun. Standards Mag.*, vol. 10, no. 2, pp. 216–225, 2026.

[3] International Telecommunication Union, "Recommendation ITU-R M.2160-0: Framework and overall objectives of the future development of imt for 2030 and beyond," 2023. [Online]. Available: https://www.itu.int/dms_pubrec/itu-r/rec/m/R-REC-M.2160-0-202311-I!!PDF-E.pdf

[4] F. Zhang *et al.*, "AFDM-enabled integrated sensing and communication: Theoretical framework and pilot design," *IEEE J. Sel. Areas Commun.*, vol. 44, pp. 310–324, 2026.

[5] A. Bemani, N. Ksairi, and M. Kountouris, "Affine frequency division multiplexing for next generation wireless communications," *IEEE Trans. Wireless Commun.*, vol. 22, no. 11, pp. 8214–8229, 2023.

[6] ETRI and University of Surrey, "Discussion on 6GR waveform & Discussion on waveform and signal for sensing," 3GPP TSG RAN WG1 contribution, status: Noted. Available from the 3GPP FTP server. [Online]. Available: https://www.3gpp.org/ftp/tsg_Ran/WG1_RL1/TSGR1_124b/Docs?sortby=sizerev

[7] 3GPP, "3GPP specification series: 38 series," Mar. 2026, accessed: 2026-03-20. [Online]. Available: https://www.3gpp.org/dynareport?code=38-series.htm

[8] A. Brodzik, "On the Fourier transform of finite chirps," *IEEE Signal Process. Lett.*, vol. 13, no. 9, pp. 541–544, 2006.

[9] V. Savaux, "Special cases of DFT-based modulation and demodulation for affine frequency division multiplexing," *IEEE Trans. Commun.*, vol. 72, no. 12, pp. 7627–7638, 2024.

[10] L. Xu, S. Sun, K. V. Mishra, and Y. D. Zhang, "Automotive FMCW radar with difference co-chirps," *IEEE Trans. Aerosp. Electron. Syst.*, vol. 59, no. 6, pp. 8145–8165, 2023.

[11] J. Zhu, Y. Tang, C. Yi, H. Yin, Y. Ni, F. Liu, Z. Wei, and H. Arslan, "ISAC with affine frequency division multiplexing: An FMCW-based signal processing perspective," Nov. 2025. [Online]. Available: https://arxiv.org/abs/2511.12308

[12] Y. Tao, M. Wen, Y. Ge, T. Mao, Y. Tang, and A. Doosti-Aref, "Affine frequency division multiple access based on DAFT spreading for next-generation wireless networks," *IEEE Trans. Wireless Commun.*, vol. 25, pp. 4626–4641, 2026.

[13] H. Yuan, Y. Xu, X. Guo, Y. Ge, T. Ma, H. Li, D. He, and W. Zhang, "PAPR reduction with pre-chirp selection for affine frequency division multiplexing," *IEEE Wireless Commun. Lett.*, vol. 14, no. 3, pp. 736–740, 2024.

[14] Q. Tao, "Precoding design for MIMO-AFDM systems: Exploiting joint spatial-affine frequency domain potential in high-mobility scenarios," *IEEE Commun. Stand. Magaz.*, pp. 1–8, 2026.

[15] Q. Luo, Z. Liu, M. Leila, T. Nikolaos, Q. Peng, and P. Xiao, "Frame-based AFDM-ISAC waveform design with chirp-enabled pulse compression," *IEEE J. Sel. Topics Signal Process.*, pp. 1–16, 2026.